

# S-Glutathionylation Regulates Inflammatory Activities of S100A9\*<sup>§</sup>

Received for publication, October 12, 2009, and in revised form, March 10, 2010. Published, JBC Papers in Press, March 11, 2010, DOI 10.1074/jbc.M109.075242

Su Yin Lim<sup>‡</sup>, Mark J. Raftery<sup>§</sup>, Jesse Goyette<sup>‡</sup>, and Carolyn L. Geczy<sup>†1</sup>

From the <sup>‡</sup>Centre for Infection and Inflammation Research and <sup>§</sup>Bioanalytical Mass Spectrometry Facility, School of Medical Sciences, University of New South Wales, Sydney, New South Wales 2052, Australia

Reactive oxygen species generated by activated neutrophils can cause oxidative stress and tissue damage. S100A8 (A8) and S100A9 (A9), abundant in neutrophil cytoplasm, are exquisitely sensitive to oxidation, which may alter their functions. Murine A8 is a neutrophil chemoattractant, but it suppresses leukocyte transmigration in the microcirculation when S-nitrosylated. Glutathione (GSH) modulates intracellular redox, and S-glutathionylation can protect susceptible proteins from oxidative damage and regulate function. We characterized S-glutathionylation of A9; GSSG and GSNO generated S-glutathionylated A8 (A8-SSG) and A9 (A9-SSG) *in vitro*, whereas only A9-SSG was detected in cytosol of neutrophils activated with phorbol myristate acetate (PMA) but not with fMLP or opsonized zymosan. S-Glutathionylation exposed more hydrophobic regions in Zn<sup>2+</sup>-bound A9 but did not alter Zn<sup>2+</sup> binding affinity. A9-SSG had reduced capacity to form heterocomplexes with A8, but the arachidonic acid binding capacities of A8/A9 and A8/A9-SSG were similar. A9 and A8/A9 bind endothelial cells; S-glutathionylation reduced binding. We found little effect of A9 or A9-SSG on neutrophil CD11b/CD18 expression or neutrophil adhesion to endothelial cells. However, A9, A9-SSG and A8/A9 promoted neutrophil adhesion to fibronectin but, in the presence of A8, A9-mediated adhesion was abrogated by glutathionylation. S-Glutathionylation of A9 may protect its oxidation to higher oligomers and reduce neutrophil binding to the extracellular matrix. This may regulate the magnitude of neutrophil migration in the extravasculature, and together with the functional changes we reported for S-nitrosylated A8, particular oxidative modifications of these proteins may limit tissue damage in acute inflammation.

Neutrophils play important roles in innate immune host defense against invading pathogens by producing a respiratory burst that generates reactive oxygen species (ROS)<sup>2</sup> via the

NADPH oxidase complex and the myeloperoxidase system (1, 2). However, excessive ROS can lead to oxidative stress, inflicting damage to cells and tissues, thereby amplifying inflammation (3). ROS also fine-tunes the inflammatory responses, depending on the circumstances of production and amounts produced (4), and can induce reversible or irreversible oxidative modifications to Cys thiols of susceptible proteins. Reversible modifications may protect proteins against permanent oxidative damage and/or modulate their functions, but excessive ROS can lead to permanent loss of function and/or cell apoptosis and necrosis that may promote pathogenesis (5).

Glutathione (GSH) is an abundant anti-oxidant in cells and plays a critical role in protection from oxidative damage (6). Protein S-glutathionylation, the disulfide coupling of a GSH moiety to Cys residues, is the prevalent S-thiolation reaction in biological systems (7–8), regulating numerous physiological processes (9). This modification may be driven by oxidative/nitrosative stress in the presence of endogenous GSH but can also persist under basal conditions and in reducing environments (10–11). It can occur via thiol-disulfide exchange with oxidized GSH (GSSG) or reaction of oxidative thiol intermediates such as S-nitrosothiols (SNO) with GSH (12). Removal of GSH is promoted by reduced thiols and changes in intracellular redox or is catalyzed by enzymes such as thioredoxin and glutaredoxin (13); reversibility is a key determinant of its physiological relevance in regulating protein function (14).

Altered levels of S-glutathionylation in some proteins are associated with pathologies such as hyperlipidemia (15), diabetes (16), Friedreich's ataxia (17), diabetes, atherosclerosis, and cancer (14), and identification of targets and their functional consequences may be clinically important. Some targets include transcription factors (Jun, NF- $\kappa$ B), enzymes (creatine kinase, human immunodeficiency virus-1 protease), and cytoskeletal proteins (actin, tubulin), all of which influence critical pathways in growth, differentiation, and metabolism (7, 12). Phagocytosis induces a respiratory burst in monocytes, resulting in S-thiolation of glyceraldehyde 3-phosphate and concomitant loss of activity (18). Glutathionylation of the p50 and p65 subunits of NF- $\kappa$ B, a transcription factor with pivotal roles in inflammation and proliferation, inhibits its binding to promoter regions of genes (19, 20). S-Thiolated actin was generated in PMA-activated neutrophils (21) and may be important in cell spreading and cytoskeletal organization (22).

A9, S100A9; VCAM-1, vascular cell adhesion molecule-1; ICAM-1, intercellular adhesion molecule 1.

\* This work was supported in part by grants from the National Health and Medical Research Council of Australia.

<sup>§</sup> The on-line version of this article (available at <http://www.jbc.org>) contains supplemental Fig. 1.

<sup>1</sup> To whom correspondence should be addressed. Tel.: 612-9385-2777; E-mail: c.gecgy@unsw.edu.au.

<sup>2</sup> The abbreviations used are: ROS, reactive oxygen species; GSH, glutathione; GSNO, S-nitrosoglutathione; GSSG, oxidized glutathione; SNO, S-nitrosothiol; AA, arachidonic acid; PMA, phorbol 12-myristate 12-acetate; fMLP, N-formyl-Met-Leu-Phe; LC, liquid chromatography; RP-HPLC, reverse phase-high performance liquid chromatography; ESI, electrospray ionization; MS, mass spectrometry; CI, cell index; IL, interleukin; PBS, phosphate-buffered saline; ANS, 1-anilino-8-naphthalene sulfonic acid; A8, S100A8;

## S100A9 Is Glutathionylated in Neutrophils after Activation

S100A8 (A8, MRP 8, calgranulin A) and S100A9 (A9, MRP 14, calgranulin B) are highly expressed in neutrophils (comprise ~40% of cytoplasmic proteins (23)) and induced in numerous cells, including monocytes (24), macrophages (25–27), and keratinocytes (28, 29) by inflammatory mediators or oxidative stress. A8 and A9 heterocomplexes (A8/A9) are secreted after neutrophil activation (30) or released as a result of necrosis (31) and have chemotactic (32), anti-microbial (33, 34), pro-apoptotic, and anti-proliferative (35, 36) activities. A9 mediates neutrophil adhesion to fibronectin, fibrinogen, and endothelial cells via activation of  $\beta 2$  integrins, suggesting a role in leukocyte transmigration (32, 37). A9 may also modulate the resolution of inflammation by suppressing macrophage activity after phagocytosis of apoptotic neutrophils (38). A9 suppressed A8-mediated NF- $\kappa$ B activation in murine bone marrow cells (39). Intracellularly, the heterocomplex transports arachidonic acid (AA) (40), which is implicated in NADPH oxidase activation (41). A9 enhances A8 binding to tubulin and A8-mediated microtubule polymerization in resting phagocytes. Phosphorylation of A9, mediated by p38 MAPK after phagocyte activation, may regulate cytoskeletal rearrangements that promote migration, a property supported by the impaired transendothelial migration of A9<sup>-/-</sup> neutrophils (42).

A8 and A9 are readily oxidized by reactive oxygen/nitrogen species, which promote structural changes that alter their functions. Oxidation of murine A8 to disulfide-linked dimers (43) or intermolecular sulfonamide-linked complexes (44) abolished its chemotactic activity and the fugetactic activity of human A8 and A9 is regulated by oxidation (45, 46). A8 and A9 are more susceptible to oxidation by HOCl than low density lipoprotein (47), and their exquisite capacity to scavenge ROS makes them primary candidates for protecting cells against oxidative stress in a localized environment. Recently, we showed that A8 and A9 are S-nitrosylated by the physiological NO donor S-nitrosoglutathione (GSNO) *in vitro*; A8 is more susceptible, and A8-SNO suppressed mast cell-mediated inflammation by reducing leukocyte adhesion and extravasation in the rat mesenteric microcirculation (48). Moreover, both proteins are up-regulated in microvascular endothelial cells by proinflammatory mediators such as IL-1 $\beta$  or tumor necrosis factor- $\alpha$  (49), and oxidative changes in the microcirculation during inflammation may alter functions of these proteins in endothelial cells.

Here we show that A9 in neutrophils is S-glutathionylated after activation. S-Glutathionylated A8 (A8-SSG) and A9 (A9-SSG) were generated with GSNO and GSSG *in vitro*, whereas only A9-SSG was detected in neutrophils activated with PMA. The single Cys<sup>3</sup> residue of A9, the site of GSH addition, is present only in the full-length form, which accounted for ~72% of total A9 in neutrophils. Structural changes in A9-SSG apparently altered its affinity for complex formation with A8 but did not affect the capacity of A8/A9 to bind AA. A9 binding to endothelial cells is implicated in their activation (50); significantly less A9-SSG and A8/A9-SSG bound HMEC-1 endothelial cells compared with the unmodified forms, likely due to differences in protein conformation. Moreover, unlike A8/A9, A8/A9-SSG did not induce neutrophil adhesion to fibronectin. We propose that glutathionylation may protect A9 from oxida-

tive damage in activated neutrophils and may limit leukocyte exudation in inflammatory lesions.

### EXPERIMENTAL PROCEDURES

**General**—Reagents and chemicals were analytical grade (Sigma; Bio-Rad), and solvents were HPLC grade (Mallinckrodt Baker). GSNO, GSH (reduced form), and GSSG were from Sigma. Recombinant human A8 and A9 and rabbit IgG raised against human A9 were produced as described (51); recombinant preparations were stored at -20 °C under argon to prevent oxidation. Liquid chromatographic separations were performed using a non-metallic LC626 HPLC system (Waters, Milford, MA) monitored at A<sub>201–280</sub> with a Waters 996 photodiode array or 490 UV-visible detector. C4 and C18 RP-HPLC columns (300 Å, 5  $\mu$ m, 250  $\times$  4.6 mm) were from Vydac, The Separations Group (Hesperia, CA).

**Generation and Characterization of A9-SSG**—A9 (50  $\mu$ g, ~3.6 nmol) was incubated with GSNO (1 mM) or GSSG (1 mM) with and without CaCl<sub>2</sub> (1 mM) or ZnCl<sub>2</sub> (50  $\mu$ M) in Tris buffer (10 mM Tris-HCl, pH 7.4) at room temperature for 1 h. Products were separated by C4 RP-HPLC in a gradient of 25–70% (v/v) CH<sub>3</sub>CN, 0.1% (v/v) trifluoroacetic acid at 1 ml/min over 25 min. Fractions with positive A<sub>214</sub> absorbance were collected and lyophilized before LC/ESI-MS analysis. To determine the site of glutathionylation by peptide mapping, C4 RP-HPLC-isolated A9 (~100  $\mu$ g) that was previously treated with GSSG or untreated was digested with endoprotease AspN (sequencing grade; Roche Applied Science) in ammonium bicarbonate (50 mM, pH 8.0, at enzyme to substrate ratio (w/w) of ~1:100) at 37 °C for 12 h. Peptide samples (5  $\mu$ l), injected into buffer A (98% (v/v) H<sub>2</sub>O, 2% CH<sub>3</sub>CN (v/v), 0.1% (v/v) formic acid), were separated on a XDB C18 column (5  $\mu$ m, 2.1  $\times$  50 mm; Agilent, Palo Alto, CA) using a linear gradient of 5–70% buffer B (20% (v/v) H<sub>2</sub>O, 80% (v/v) CH<sub>3</sub>CN, 0.1% (v/v) formic acid) at 150  $\mu$ l/min over 20 min, and fractions at A<sub>214</sub> were collected for LC/ESI-MS analysis.

**Isolation of Full-length and Truncated (A9\*) A9 and A9-SSG from Neutrophils**—Human neutrophils (2  $\times$  10<sup>7</sup>/ml) were isolated from citrated blood from five individual donors using density gradient centrifugation with Ficoll-Paque Plus (GE Healthcare). Cells were lysed by three freeze/thaw cycles in 100  $\mu$ l of PBS and centrifuged at 14,000  $\times$  g for 5 min, and supernatants were immediately separated by C4 RP-HPLC in a gradient of 40–55% (v/v) CH<sub>3</sub>CN, 0.1% (v/v) trifluoroacetic acid over 25 min to achieve partial separation of the two isoforms. Major fractions at A<sub>214</sub> were collected for LC/ESI-MS analysis, and relative concentrations of the two isoforms were calculated by comparison of peak areas over total protein peak area of all HPLC fractions.

Neutrophils (4  $\times$  10<sup>6</sup>/ml) were incubated with 1  $\mu$ g/ml PMA (Sigma), 1  $\mu$ g/ml ionomycin (Sigma), 1 mM EDTA (Sigma), or the combination in PBS (25 mM phosphate, 250 mM NaCl, pH 7.5) at 37 °C for 15 min and harvested by centrifugation. Alternatively, neutrophils were incubated with 1  $\mu$ M N-formyl-Met-Leu-Phe (fMLP; Sigma) or opsonized zymosan (0.5 mg/ml prepared according to Markert *et al.* (52); Sigma) for 15 min at 37 °C. Neutrophil cytosol was separated by C4 RP-HPLC in a gradient of 25–75% (v/v) CH<sub>3</sub>CN, 0.1% (v/v) trifluoroacetic acid

over 25 min to ensure separation of A9 from A8. Major fractions at  $A_{214}$  were collected and lyophilized for LC/ESI-MS analysis.

Some mass spectra were acquired using a QStar MS system equipped with a nano-ESI source (QStar Pulsar *i*, Applied Biosystems, Foster City, CA; mass accuracy of <50 ppm). Because the many HPLC fractions from neutrophil lysate samples would require an extensive number of MS runs, masses of proteins from these samples were determined using LC/MS with single quadrupole MS (1100 MSD; Agilent, San Jose, CA). Nitrogen was the nebulizer gas, and samples were ionized at a positive potential of 4 kV, then transferred to the mass analyzer with a fragmentor voltage (capillary to skimmer lens voltage) of 225 V. Spectra were acquired over  $m/z$  600–2000, with a cycle time of 2 s. Each series of multiple-charged ion was deconvoluted using the manufacturer's software (Chemstation Version A.09.01), with a mass accuracy of  $\pm 0.01\%$ .

**Immunofluorescence Staining**—To examine the possibility that A9-SSG translocates to specific cellular structures after activation, neutrophils ( $2 \times 10^6$ /ml) untreated or treated with 1  $\mu$ g/ml PMA plus ionomycin, 1  $\mu$ M fMLP, or 0.5 mg/ml opsonized zymosan in PBS for 15 min at 37 °C were diluted 1:10 (v/v) in 50% (v/v) BCS (Invitrogen)/RPMI 1640 and centrifuged onto glass slides at 500 rpm for 5 min using a Cytospin 3 cytocentrifuge (Shandon Life Sciences, Astmor, UK). Samples were fixed with 4% (w/v) paraformaldehyde in PBS, permeabilized with PBS containing 0.5% (w/v) saponin and 0.1% (w/v) bovine serum albumin, and then blocked with 1% (w/v) bovine serum albumin in PBS for 1 h. For double immunofluorescence, cells were incubated with anti-A9 IgG (5  $\mu$ g/ml) or normal rabbit IgG (5  $\mu$ g/ml) together with murine monoclonal antibodies against GSH (5  $\mu$ g/ml; Abcam, Cambridge, MA) or isotype control (5  $\mu$ g/ml) for 2 h at room temperature. After washing with PBS, cells were incubated with Alexa 488-conjugated anti-mouse IgG and Alexa 568-conjugated anti-rabbit IgG (1:200, Molecular Probes, Eugene, OR) for 1 h in the dark, washed, and nuclei-stained with 4',6'-diamidino-2-phenylindole (0.3  $\mu$ M in PBS; Sigma) for 10 min. Confocal microscopy was performed using an Olympus FV1000 inverted microscope, and images were processed using Adobe Photoshop 9.0 (Adobe Systems Inc.).

**Ion Binding Activity of A9 and A9-SSG**—The 1-anilino-8-naphthalene sulfonic acid (ANS) fluorimetry was used to evaluate whether glutathionylation of A9 affected its ion binding capacity. ANS (60  $\mu$ M) was added to A9 or A9-SSG (20  $\mu$ M) in Tris buffer in 96-well plates (Greiner) with 1 mM EDTA, 1 mM  $\text{CaCl}_2$ , 50  $\mu$ M  $\text{ZnCl}_2$ , or the combination. For  $\text{Zn}^{2+}$  titration studies, increasing concentrations of  $\text{ZnCl}_2$  (0–150  $\mu$ M) were used, and emission spectra were measured at 10-nm intervals between 420–600 nm, with an excitation wavelength of 385 nm on a SpectraMax spectrophotometer (Molecular Devices, Sunnyvale, CA) using SoftMaxPro software. GraphPad Prism (V5 Windows GraphPad, San Diego, CA) was used to fit non-linear regression curves using the Hill equation. Values are reported as relative ANS-A9 fluorescence after background subtraction of ANS with divalent cations or EDTA.

**AA Binding Capacity of A8/A9 and A8/A9-SSG**—To determine whether glutathionylation of A9 affected its AA binding

capacity, A8 and A9 or A9-SSG (100  $\mu$ M) were incubated with 50  $\mu$ M AA, and binding was carried out as described (53) with some modifications. Supernatants (200  $\mu$ l) of samples after incubation with 50% (v/v) hydroxyalkoxypropyl dextran type VI (Sigma) suspension to remove unbound AA were separated by C18 RP-HPLC in a gradient of 40–80% (v/v)  $\text{CH}_3\text{CN}$ , 0.1% (v/v) trifluoroacetic acid over 50 min. HPLC separation of A8, A9/A9-SSG, and AA generated peaks absorbing at  $A_{214}$  that were collected for LC/ESI-MS analysis. Relative abundance of AA, A8, A9, or A9-SSG was determined from the calculated area of their corresponding peaks. AA binding affinities of A8/A9 and A8/A9-SSG were assessed as the ratio of peak area of bound AA over peak area of A8.

**Expression of  $\beta 2$  Integrin and Neutrophil Adhesion**—To examine the effect of A9 glutathionylation on  $\beta 2$  integrin expression, human dextran-sedimented white blood cells (1 ml) from 6 individual donors were washed twice in 20 mM HEPES, pH 7.5, in HBSS containing 1 mM  $\text{Ca}^{2+}$ , 1 mM  $\text{Mg}^{2+}$ , and 10  $\mu$ M  $\text{Zn}^{2+}$  before incubation ( $\sim 5 \times 10^4$  cells; 50  $\mu$ l) with A9, A9-SSG, or fMLP (1  $\mu$ M) for 30 min at 37 °C. Phycoerythrin-conjugated anti-CD11b (BD Biosciences), anti-CD18 (BD Biosciences), anti-CBRM (activation-specific CD11b epitope; eBiosciences, San Diego, CA) antibodies or appropriate IgG isotype controls (BD Biosciences) were added for 15 min at room temperature, and cells were washed and fixed in 2% (w/v) paraformaldehyde and analyzed using a FACScan flow cytometer (BD Biosciences). In all experiments 10,000 events were collected from a large gate that included polymorphonuclear cells but excluded monocytes, lymphocytes, and debris.

A9 induces neutrophil adhesion to fibronectin (37), and to investigate if glutathionylation affected this, the Real-time Cell Analyzer xCELLigence system (Roche Applied Science) was used to monitor neutrophil adhesion (54). 96-well E-Plates, which contain electrodes that measure cell index (CI) based on impedance (CI correlates with the number of cells attached) (54), were coated with 50  $\mu$ g/ml fibronectin (Sigma), incubated at 4 °C overnight, then blocked with 1% (w/v) bovine serum albumin/PBS for 2 h. Neutrophils ( $5 \times 10^6$  cell/ml) from 3 individual donors were treated with A8, A9, A9-SSG, A8/A9, A8/A9-SSG (1 and 2.5  $\mu$ M), or fMLP (1 and 2.5  $\mu$ M) in 1% (w/v) bovine serum albumin/RPMI 1640 and immediately transferred to each well (100  $\mu$ l/well;  $5 \times 10^4$  neutrophils/well). CI was measured every 15 s for 2 h and directly relates to the numbers of neutrophils that adhered to fibronectin. Treatments were performed in triplicate; mean CI values  $\pm$  S.D. were obtained using Real-time Cell Analyzer Software 1.2 (Roche Applied Science).

Effect of A9 and A9-SSG on Neutrophil Adhesion to HMEC-1 Microvascular Endothelial cells (provided by Prof. L. M. Khachigian, University of New South Wales) was investigated. HMEC-1 were cultured in MCDB 131 media (Invitrogen) supplemented with 10% (v/v) fetal bovine serum, 10 ng/ml epidermal growth factor (Sigma), and 1  $\mu$ g/ml hydrocortisone (Sigma) (55) in 96-well plates, and neutrophil binding was assayed as described (32).

**A9 and A9-SSG Binding and Activation of HMEC-1**—A9 and A8/A9 are reported to bind and activate endothelial cells (50), and to investigate the effect of A9 glutathionylation on binding,

## S100A9 Is Glutathionylated in Neutrophils after Activation

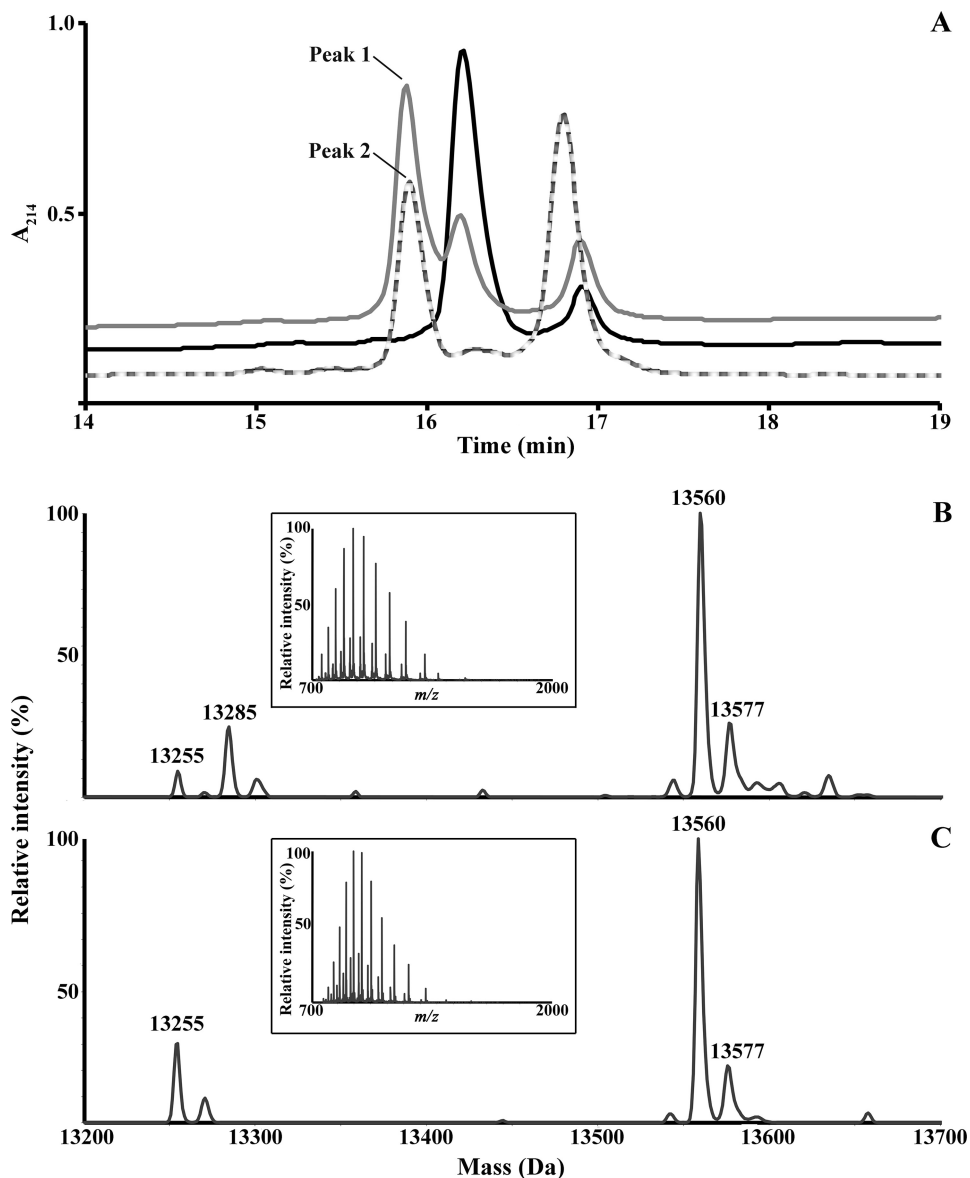


**FIGURE 1. Characterization of A9-SSG.** *A*, two peaks with retention times of 16.3 min and 16.9 min were observed when recombinant human A9 (black) was separated by C4 RP-HPLC. Separation of GSNO- (gray) and GSSG-treated (dashed line) A9 generated an additional peak with retention time of 15.95 min (peaks 1 and 2, respectively). Deconvoluted masses were derived from the ESI mass spectra (insets) of multiply charged ions of peaks 1 (*B*) and 2 (*C*). In GSNO-treated A9, masses corresponding to A9 (13,255 Da) and likely to A9-SNO (13,285 Da; +30 Da) were observed. GSNO and GSSG both generated a major component of 13,560 Da, equivalent to the theoretical mass of A9-SSG, and a minor component of 13,577 Da, that may correspond to oxidation of a single Met residue in A9-SSG.

A8, A9, A9-SSG, A8/A9, or A8/A9-SSG ( $1 \mu\text{M}$ ) were incubated with HMEC-1 in 96-well plates for 2 h at  $37^\circ\text{C}$ . Plates were washed, incubated with biotinylated anti-human A9 IgG ( $5 \mu\text{g/ml}$ ) in PBS for 1 h, and developed as described (48).  $A_{450}$  was measured (Titertec Multiscan MCC/340; LabSystem, Helsinki, Finland), and data were normalized to the total absorbance of each experiment after background subtraction.

To determine whether A9-SSG altered expression of some inflammation-associated genes reported to be induced by A9 (50), HMEC-1 were plated onto 12-well plates ( $2.5 \times 10^5/\text{well}$ ), grown to confluence, and stimulated with A8, A9, A9-SSG, A8/A9, A8/A9-SSG ( $20 \mu\text{M}$ ), tumor necrosis factor- $\alpha$  ( $25 \text{ ng/ml}$ ), or media control for 6, 12, or 24 h before extracting total

RNA with Trizol (Invitrogen). RNA was isolated, and real time reverse transcription-PCR was performed as described (26) using the following primers:  $\beta$ -actin, 5'-CATGTA-CGTTGCTATCCAGGC-3' and 5'-CTCCTTAATGTCACGCAC-GAT-3'; IL-8, 5'-GCCTTCCTG-ATTTCTGCAGCT-3' and 5'-T-GCACTGACATCTAAGTTCTT-TAGCAC-3', ICAM-1, 5'-AGA-GGTCTCAGAAGGGACCG-3' and 5'-GGGCCATACAGGACA-CGAAG-3'; VCAM-1, 5'-GCTGC-TCAGATTGGAGACTCA-3' and 5'-CGCTCAGAGGGCTGTCT-ATC-3'. Relative mRNA levels in duplicate samples were obtained using the  $\Delta C_T$  method and normalized to  $\beta$ -actin as the endogenous control.

**Statistical Analysis**—Data were analyzed using analysis of variance (ANOVA) (or repeated measures ANOVA when neutrophils from different blood donors were used) followed by Dunnett's post-test to compare differences between treatment and control or by the Bonferroni post-test for multiple comparisons. All values are reported as the means  $\pm$  S.D. Statistical significance was set at  $p < 0.05$ .

## RESULTS

**Characterization of A9-SSG**—Recombinant A9 treated with GSNO or GSSG was eluted from C4 RP-HPLC, and masses were determined. Both generated an additional component with a retention time of 15.95 min compared with untreated A9, which contained two components (Fig. 1*A*), the masses of which corresponded to A9 monomer (retention time 16.3 min) and disulfide-linked dimer (retention time 16.8 min). This indicated some spontaneous oxidation of A9, and GSSG treatment increased relative abundance of the dimer (retention time, 16.8 min).

The deconvoluted ESI mass spectra (insets) of the uncharacterized component generated by GSNO (Fig. 1*B*) or GSSG (Fig. 1*C*) indicated a major product of 13,560 Da, identical to the theoretical mass addition of GSH (+307 Da) and subsequent loss of two hydrogen molecules ( $-2 \text{ Da}$ ) on recombinant A9 (13,255 Da). An additional modification, likely corresponding to A9-SNO (13,285 Da), with mass addition of NO and loss of a hydrogen molecule (+29 Da) was also generated by GSNO

## S100A9 Is Glutathionylated in Neutrophils after Activation

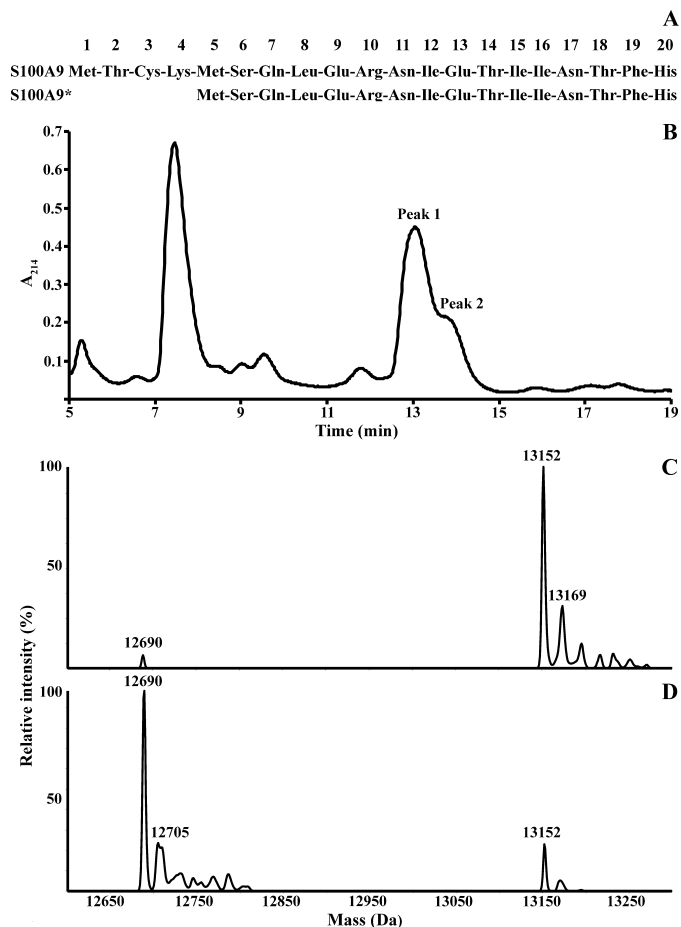


**FIGURE 2. C4 RP-HPLC separation of A9 (retention time, 13.1 min; peak 1) and A9\* (retention time 14 min; peak 2) from neutrophil cytosol.** *A*, shown are the first 20 N-terminal amino acid residues of A9 and A9\* protein sequences, depicting the start Met (Met<sup>1</sup> and Met<sup>5</sup>). *B*, a representative chromatogram of one of five donors is shown. The deconvoluted mass spectrum of peak 1 (*C*) indicated a major component of 13,152 Da, corresponding to A9. The major component of the deconvoluted mass spectrum of peak 2 (*D*) indicated a molecular mass of 12,690 Da, corresponding to A9\*. Components with masses of 13,169 Da and 12,705 Da likely correspond to oxidation of a single Met residue in A9 and A9\*, respectively.

treatment, although A9-SSG was more abundant (ratio 1:3.75) (Fig. 1*B*). MS analysis of the A9<sub>1-30</sub>-SSG peptide, generated after AspN digestion of A9-SSG, indicated a mass increase of 305 Da (3737 Da) compared with the theoretical mass of A9<sub>1-30</sub> (3431 Da) (not shown), suggesting the site of glutathionylation to be Cys<sup>3</sup>. Other modifications were mass additions of 16 and 321 Da, likely corresponding to oxidation of a single Met residue to methionine sulfoxide in A9 (13271 Da; Fig. 1*C*) and A9-SSG (13577 Da; Fig. 1, *B* and *C*). A9-SSG products were generated in similar yields when A9 was treated with GSSG in the presence of Ca<sup>2+</sup> and/or Zn<sup>2+</sup>. GSH (1 mM) spontaneously converted Cys<sup>3</sup>-A9-SSG to the natural A9 monomer with ~65% conversion within 1 h (not shown).

**Relative Abundance of A9 and A9\* in Neutrophils**—Two isoforms of A9, the full-length and the truncated (A9\*) form (Fig. 2*A*), are found in neutrophils, the latter generated from an alternate translation start site at Met<sup>5</sup> (56), but there is no information concerning their relative abundance. The isoforms were partially resolved by C4 RP-HPLC, with retention times of 13.1 min (*peak 1*) and 14 min (*peak 2*) (Fig. 2*B*). The deconvoluted

ESI mass spectra of peak 1 (Fig. 2*C*) and peak 2 (Fig. 2*D*) indicated components of 13,152 and 12,690 Da, identical to the theoretical masses of A9 after removal of the N-terminal Met residue and acetylation of Thr<sub>2</sub>, and of A9\* after the N-terminal Met removal and Ser<sup>6</sup> acetylation as described (57). Masses likely corresponding to Met oxidation on A9 (13,169 Da) and A9\* (12,705 Da) were also detected. To determine the relative abundance of A9 and A9\*, neutrophil cytosol from 5 healthy donors was separated, and areas under the HPLC peaks indicated that full-length A9 was the predominant form, constituting  $71.9 \pm 1.05\%$  of total A9.

**S-Glutathionylation of A9 Is Generated by Neutrophil Activation**—A8 and A9 in neutrophil cytosol were readily separated by C4 RP-HPLC, with retention times of 15 and 16 min, respectively (Fig. 3*A*). PMA (Fig. 3*B*) or PMA plus ionomycin (Fig. 3*C*) treatment generated additional components with retention time of 15.7 min (Fig. 3*A*, †). The ESI mass spectra (*insets*) of these, when deconvoluted, contained products with masses of 13,152 and 13,457 Da, likely corresponding to A9 and A9-SSG (mass addition of GSH (+307 Da), and loss of two hydrogen molecules (-2 Da)). Retention times and masses of native A9 and A9-SSG were different from those of the recombinant proteins (Fig. 1, *B* and *C*) because of the additional Gly and Ser residues engineered to produce a thrombin cleavage site in the recombinant protein (51) and the post-translational processing in the native protein (57).

Additional A9 adducts were also generated; masses and proposed modifications are shown in Table 1. These may correspond to cysteinylated (13,272 Da; +120 Da) after activation with PMA plus ionomycin, oxidation of a single Met residue in A9 to methionine sulfoxide (13,168 Da; +16 Da) or Met sulfone (13,185 Da; +33 Da), phosphorylation of a single residue and methionine sulfoxide (13,249 Da; +97 Da), and an uncharacterized modification of +283 Da. Products with masses corresponding to A9-SSG were not found in the cytosol of untreated neutrophils or those treated with ionomycin alone, although possible A9 modifications in ionomycin-treated neutrophils included methionine sulfoxide and sulfone and disulfide-linked A9 (not shown). Contrary to earlier studies (58), we found no evidence of A9 phosphorylation (theoretical mass addition of 80 Da) promoted by ionomycin.

fMLP or opsonized zymosan generated several modifications in A9, although products with masses corresponding to A9-SSG were not detected. Products with masses possibly corresponding to phosphorylated A9, Met oxidation to methionine sulfoxide and sulfone, and the disulfide-linked dimer were found in preparations from fMLP-treated neutrophils. Opsonized zymosan predominantly generated products that likely corresponded to disulfide-linked A9 dimer. Some products with masses similar to phosphorylated A9 and Met sulfone were detected in low abundance (Table 2).

**Co-localization of A9 and GSH in Activated Neutrophils**—A9 translocates with A8 from the cytoplasm to cytoskeletal components in the plasma membrane of phagocytes after stimulation with agents that increase [Ca<sup>2+</sup>]<sub>i</sub> (59, 60) and/or promote activation (61). Immunofluorescence staining was performed to investigate possible A9 co-localization with GSH in neutrophils and whether glutathionylation was co-incidental with

## S100A9 Is Glutathionylated in Neutrophils after Activation

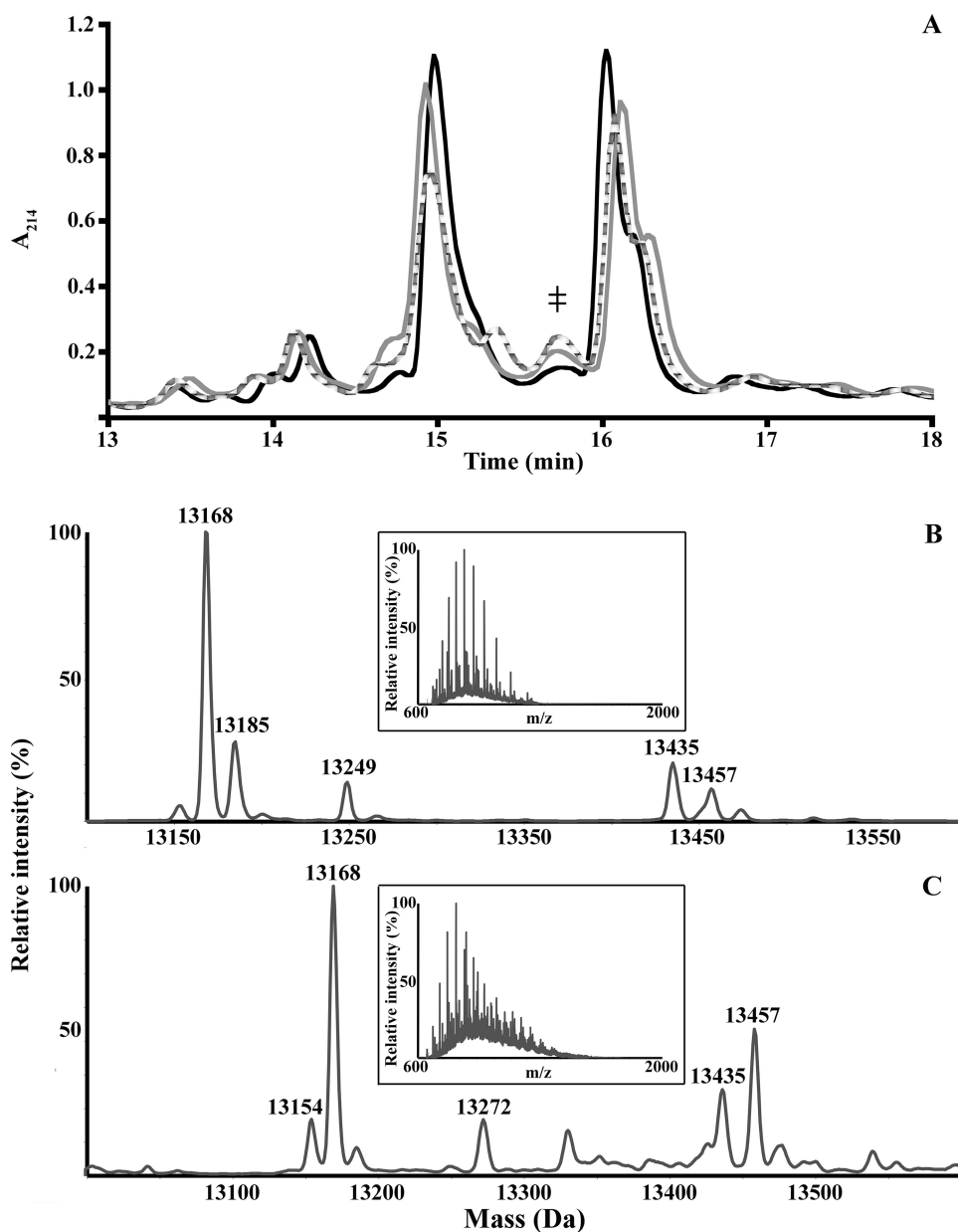


**FIGURE 3. C4 RP-HPLC separation of neutrophil cytosol and identification of A9 adducts.** *A*, an additional component ( $\ddagger$ ) with a retention time of 15.7 min was generated when cytosol of neutrophils treated with PMA (gray) or PMA plus ionomycin (dashed line) were separated and compared with untreated (black) cells. Several A9 adducts (Table 1) were observed when the ESI mass spectra (insets) of the peak ( $\ddagger$ ) from PMA (*B*)- and PMA plus ionomycin (*C*)-treated neutrophils were deconvoluted. A component of 13,457 Da was observed in both and may correspond to A9-SSG. Results are representative of separations of neutrophil cytosol preparations from three normal donors.

**TABLE 1**

The deconvoluted masses of A9 adducts and their proposed modifications from ESI mass spectra of PMA- and PMA plus ionomycin-treated neutrophils

PMA-treated neutrophils		PMA + ionomycin-treated neutrophils	
Mass	Possible modifications	Mass	Possible modifications
<i>Da</i>		<i>Da</i>	
13,152	Full-length A9	13,152	Full-length A9
13,168	+ 16 Da; oxidation to Met sulfoxide	13,168	+ 16 Da; oxidation to Met sulfoxide
13,185	+ 33Da; oxidation to Met sulfone	13,272	+ 120 Da; cysteinylatation
13,249	+ 97 Da; phosphorylation and oxidation to Met sulfoxide	13,435	+ 283 Da; unknown modification
13,435	+ 283 Da; unknown modification	13,457	+ 305 Da; glutathionylation
13,457	+ 305 Da; glutathionylation		

**A** translocation of A9 in activated cells. Strong red fluorescence was evident in the cytoplasm of untreated neutrophils stained with anti-A9 IgG (Fig. 4A, upper panel), consistent with its high constitutive expression in these cells (62). Strong GSH reactivity (green fluorescence, Fig. 4A, middle panel) was also detected, in agreement with the expected high intracellular GSH concentrations (63). The merged image (Fig. 4A, lower panel) shows some overlapping A9 and GSH reactivity in the cytoplasm and around the cell membrane. The anti-GSH antibodies (Abcam) recognize free intracellular GSH and glutathionylated protein complexes, and co-localization of staining may indicate low levels of glutathionylated A9 complexes in unstimulated neutrophils. However, A9-SSG was not detected in untreated neutrophils by ESI-MS but may have been generated transiently or as a consequence of neutrophil adhesion during slide preparation or be present in amounts below the level of detection using ESI-MS. No reactivity (inset, Fig. 4A) was apparent in neutrophils stained with rabbit IgG and IgG2a isotype control.

Contrary to studies reporting  $\text{Ca}^{2+}$ -dependent translocation of A9 to the plasma membrane in activated phagocytes (64), no changes in staining patterns were observed in neutrophils treated with PMA plus ionomycin or fMLP compared with untreated cells. A9 and GSH reactivity (red and green fluorescence, respectively) was seen in the cytoplasm and around the cell membrane (Fig. 4B) of PMA and ionomycin-treated neutrophils, and

**TABLE 2**

The deconvoluted masses of A9 adducts and their proposed modifications from ESI mass spectra of fMLP- and opsonized zymosan-treated neutrophils

fMLP-treated neutrophils		Opsonized zymosan-treated neutrophils	
Mass	Possible modifications	Mass	Possible modifications
<i>Da</i>		<i>Da</i>	
13,152	Full-length A9	13,152	Full-length A9
13,231	+80; phosphorylation	13,179	+27; unknown modification
13,168	+16; oxidation to Met sulfoxide	13,231	+80; phosphorylation
13,200	+49; oxidation to Met sulfoxide and sulfone	26,305	+13152; dimeric A9
13,230	+90; unknown modification	26,384	+13231; dimeric A9 and phosphorylation

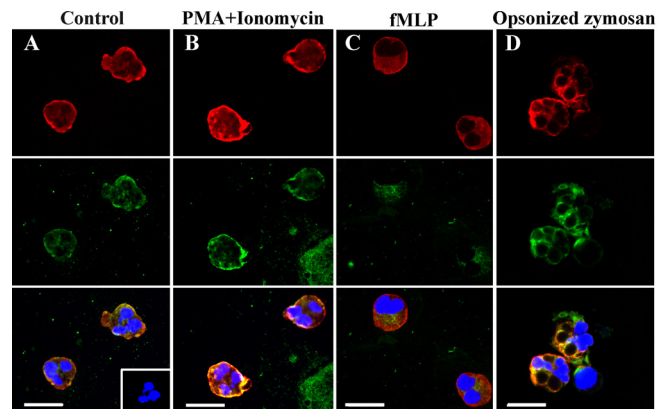


**FIGURE 4. Immunofluorescence staining of A9 and GSH in neutrophils.** A, A9 (upper panels; red) and GSH (middle panels; green) were detected in resting neutrophils, predominantly in the cytoplasm, and around the cell membrane. An overlay of the two images (lower panels) with 4',6'-diamidino-2-phenylindole staining for nuclei (blue) indicates co-localization of A9 with GSH. Negative control antibodies, rabbit IgG, and IgG2a isotype control, showed no background fluorescence (inset). B, A9 and GSH were detected in the cytoplasm and around the cell membrane of PMA plus ionomycin-treated neutrophils; the merged image indicates co-localization of A9 with GSH. C, A9 was observed in the cytoplasm and around the cell membrane of fMLP-treated neutrophils, whereas GSH was mainly cytoplasmic, and little co-localization was obvious. D, in neutrophils activated by opsonized zymosan, A9 and GSH were located predominantly around the cell membrane and the phagosome containing zymosan. The merged image indicates co-localization of A9 with GSH. Scale The bar = 28  $\mu\text{m}$ ; magnification, 1000 $\times$ . Results are representative of cells from two donors that had undergone the same treatments.

the merged image (Fig. 4B, lower panel) indicates strong co-localization of A9 with GSH. Similar A9 reactivity was observed in fMLP-treated neutrophils (Fig. 4C, upper panel), although the staining intensity for GSH was less (Fig. 4C, middle panel), and the merged image (Fig. 4C, lower panel) indicates little co-localization of A9 and GSH reactivity, which was principally intracytoplasmic.

When neutrophils were activated with opsonized zymosan, A9 (Fig. 4D, upper panel) and GSH (Fig. 4D, middle panel) localized around the zymosan, possibly in phagosomal membranes. Although A9-SSG was not detected in neutrophils treated with opsonized zymosan, the strong overlap of A9 and GSH reactivity in the merged image (Fig. 4D, lower panel) suggests co-localization, possibly associating with membrane components that would not have been present in the cytosolic fraction used for separation and ESI-MS analysis.

**Ion Binding Affinity of A9 and A9-SSG**—S100B and S100A1 are susceptible to glutathionylation (65), and S100A1-SSG had increased affinity for  $\text{Ca}^{2+}$  (66). To address whether A9 glutathionylation altered its ion-bound structure and its affinity for bivalent cations,  $\text{Ca}^{2+}$ - and  $\text{Zn}^{2+}$ -dependent changes in the hydrophobic matrices of A9 and A9-SSG were determined

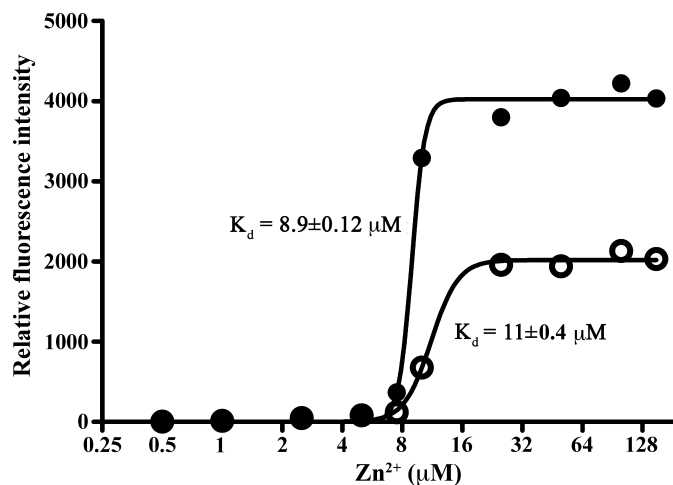


**FIGURE 5.  $\text{Zn}^{2+}$ -induced structural changes in A9 and A9-SSG.** A larger change in fluorescence intensity was observed in A9-SSG (●) compared with A9 (○) upon the addition of increasing doses of  $\text{Zn}^{2+}$ .  $\text{Zn}^{2+}$  binding affinities of the two forms were similar; A9-SSG had a  $\text{Zn}^{2+}$  binding constant ( $K_d$ ) of  $8.9 \pm 0.1 \mu\text{M}$ , and A9 had a  $K_d$  of  $11 \pm 0.4 \mu\text{M}$ . Results shown are the averages of duplicate wells and are representative of three experiments.

using ANS fluorescence. Compared with the apo (unbound) forms,  $\text{Ca}^{2+}$ -bound A9 and A9-SSG showed similar increases in fluorescence, indicating that  $\text{Ca}^{2+}$  binding induced similar conformational changes in the tertiary structures of both forms (not shown). In contrast, the larger increase in fluorescence observed for  $\text{Zn}^{2+}$ -bound A9-SSG compared with  $\text{Zn}^{2+}$ -bound A9 (Fig. 5) indicates that  $\text{Zn}^{2+}$ -induced conformational changes in A9-SSG likely exposed more hydrophobic regions on the protein surface compared with those generated with A9. Effects were additive with increasing concentrations of  $\text{Zn}^{2+}$ . A9 had a  $\text{Zn}^{2+}$  disassociation constant ( $K_d$ ) of  $11 \pm 0.4 \mu\text{M}$ , and A9-SSG had a similar  $K_d$  value of  $8.9 \pm 0.1 \mu\text{M}$  (Fig. 5), suggesting no apparent difference in their  $\text{Zn}^{2+}$  binding affinities.

**AA Binding Affinity of A8/A9 and A8/A9-SSG**—The  $\text{Ca}^{2+}$ -dependent interaction of A8/A9 with AA is specific for the heterocomplex and is inhibited by  $\text{Zn}^{2+}$  and  $\text{Cu}^{2+}$  (41, 67), possibly because these ions induce structural changes that regulate AA binding. Considering the structural differences in  $\text{Zn}^{2+}$ -bound A9-SSG and A9, we examined if AA binding was affected but found that A8/A9 and A8/A9-SSG bound AA with similar capacities (not shown).

**Effect of A9 and A9-SSG on Integrin-dependent Neutrophil Adhesion to Fibronectin and HMEC-1**—A9-SSG may be secreted after neutrophil activation or released by necrotic neutrophils and may mediate specific extracellular processes. Given the highly oxidizing conditions in the extracellular space in inflammation, A9-SSG may remain relatively stable and may

## S100A9 Is Glutathionylated in Neutrophils after Activation

have functions distinct from A9. Because A9 is reported to up-regulate  $\beta 2$  integrins CD11b and CD18 (the Mac-1 complex) on neutrophil surface (32, 37) and to promote expression of a high affinity "activation-specific epitope" (CBRM) on CD11b (68), we investigated whether glutathionylation altered these functions. Compared with untreated cells, the mean channel fluorescence of CD11b, CD18, and CBRM increased when leukocytes were stimulated with fMLP, confirming up-regulation and activation of CD11b and CD18 (Fig. 6A, \*,  $p < 0.05$ ). Stimulation of leukocytes with A9 or A9-SSG ( $n = 6$ ; separate donors) generated smaller increases that were not significant compared with untreated controls (Fig. 6A); neutrophils from 3–6 donors responded weakly to A9, and glutathionylation did not affect these.

A9 also promotes neutrophil adhesion to fibronectin via  $\beta 2$  integrin activation (37), and although we found no significant up-regulation of CD11b/CD18, we tested whether glutathionylation of A9 altered adhesion. Real-time analysis of neutrophil adhesion to fibronectin using the xCELLigence system (supplemental Fig. 1) showed dramatic linear increases in the CI of neutrophils treated with fMLP, A9, A9-SSG, or A8/A9; maximal CI, indicative of saturated adhesion, was observed ~1 h after neutrophil treatment. On the other hand, neutrophils treated with A8/A9-SSG or A8 had low CIs with little obvious increase compared with untreated cells. The compiled data from three donors indicated that fMLP significantly increased neutrophil adhesion to fibronectin in a dose-dependent manner compared with control (Fig. 6B; \*,  $p < 0.01$ ). A9 and A9-SSG also dose-dependently increased adhesion to levels comparable with those induced by fMLP (Fig. 6B; \*,  $p < 0.01$ ). A8 had no effect. A8/A9 promoted neutrophil adhesion to fibronectin to levels similar to those induced by A9 or A9-SSG (\*,  $p < 0.01$ ), indicating that A8 did not modulate the effect of A9. In marked contrast, A8/A9-SSG failed to promote adhesion, and levels were significantly less than those of A8/A9 (Fig. 6B; \*\*,  $p < 0.01$ ) and not significantly higher than untreated control.

We also investigated if A9 glutathionylation affected neutrophil adhesion to HMEC-1 cells and found that A9, A9-SSG, A8/A9, and A8/A9-SSG promoted only slight and statistically insignificant adhesion, inducing an ~3-fold less neutrophil adhesion compared with fMLP. A8 had no effect (not shown).

**Effect of A9 and A9-SSG on HMEC-1 Cells**—A8 and A9 may be deposited onto the endothelium by extravasating leukocytes (69), and A9 binds endothelial cells in a  $Ca^{2+}$ - and  $Zn^{2+}$ -dependent manner via heparin and heparan sulfate proteoglycans (69, 70) and/or carboxylated *N*-glycans (71). Because A9-SSG was generated in activated neutrophils, we investigated if glutathionylation affected its capacity to bind HMEC-1 cells. A9, A9-SSG, A8/A9, and A8/A9-SSG binding was detected using biotinylated anti-A9 IgG. Significantly more A9 and A8/A9 bound compared with A9-SSG and A8/A9-SSG (Fig. 7A; \*,  $p < 0.01$ ), indicating that glutathionylation reduced A9 binding capacity. Somewhat more A8/A9 and A8/A9-SSG heterocomplexes bound HMEC-1 than the individual A9 subunits, in accordance with published results showing higher binding affinity of the complex (55). A9 binding to endothelial cells is implicated in regulation of leukocyte migration, possibly by

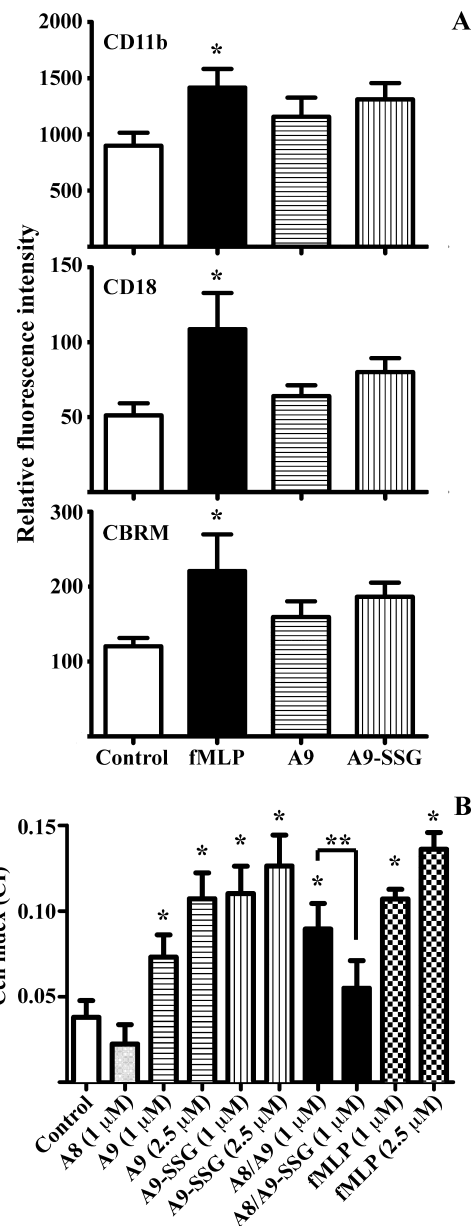


**FIGURE 6. A9 and A9-SSG induce integrin-dependent neutrophil adhesion to fibronectin.** A, treatment of dextran-sedimented white blood cells with fMLP (1  $\mu$ M; black bars) significantly increased expression of CD11b, CD18, and CBRM (\*,  $p < 0.05$ ) compared with untreated controls (white bars), assessed by flow cytometry. A9 (horizontal bars) and A9-SSG (vertical bars) treatments increased CD11b, CD18, and CBRM expression, but effects were not significant when compared with untreated controls. Values represent the mean fluorescence intensities  $\pm$  S.D. of neutrophils from six donors; quantitation is given under "Experimental Procedures." B, fMLP (checkered bars), A9 (horizontal bars), and A9-SSG (vertical bars) significantly induced neutrophil adhesion to fibronectin in a dose-dependent manner. A8/A9 (black bar) also stimulated neutrophil adhesion, but A8/A9-SSG (dark gray bar) and A8 (light gray bar) had no effect. Data represent CI values  $\pm$  S.D. of neutrophils from three donors; quantitation is given under "Experimental Procedures." \*,  $p < 0.01$ , fMLP, A9, A9-SSG, and A8/A9 compared with the untreated control; \*\*,  $p < 0.01$ , A8/A9-SSG compared with A8/A9.

inducing adhesion molecules (50). Hence, we investigated if A9-SSG affected ICAM-1 and VCAM-1 expression on HMEC-1. Tumor necrosis factor- $\alpha$  increased ICAM-1 and VCAM-1 mRNA > 1000-fold and IL-8 mRNA > 100-fold compared with untreated control (Fig. 7B; \*,  $p < 0.01$ ). However, in contrast to the previous report (50), we found no ICAM-1,

## S100A9 Is Glutathionylated in Neutrophils after Activation

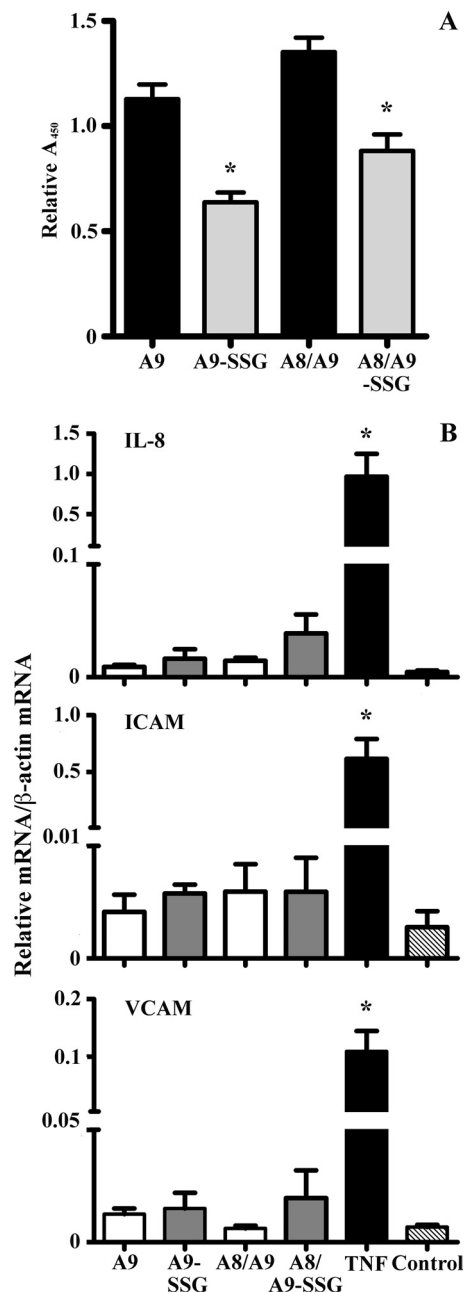


**FIGURE 7. Effect of A9, A9-SSG, A8/A9, and A8/A9-SSG on HMEC-1 binding and activation.** *A*, significantly more A9 and A8/A9 (black bars) bound HMEC-1 cells than their glutathionylated forms (A9-SSG and A8/A9-SSG; gray bars). Data are normalized to total mean absorbance and represent the means  $\pm$  S.D. of duplicate measurements from five experiments; quantification is given under "Experimental Procedures."  $^*p < 0.01$ , A9-SSG compared with A9, and A8/A9-SSG compared with A8/A9. *B*, IL-8, ICAM-1, and VCAM-1 mRNA were induced in HMEC-1 cells treated with fMLP but not with A8, A9, A9-SSG, A8/A9, or A8/A9-SSG. HMEC-1 cells were harvested 6 h post-treatment, and mRNA levels were quantitated. Data are normalized to  $\beta$ -actin and represent the means  $\pm$  S.D. of triplicate measurements of at least two experiments.  $^*p < 0.05$ , fMLP compared with untreated control. *TNF*, tumor necrosis factor- $\alpha$ .

VCAM-1, or IL-8 induction by A9 or A8/A9 and no effect of A9-SSG or A8/A9-SSG (Fig. 7*B*).

### DISCUSSION

Responses of cells to oxidative stress typically involve changes in thiol content, and *S*-thiolation is an important pro-

TECTIVE mechanism that can regulate functions of susceptible proteins (9, 72). A8 and A9, abundant in neutrophil cytosol, are extremely sensitive to oxidation by reactive oxygen/nitrogen species (43, 47–48), and oxidative modifications alter several functions (43–45, 73); we proposed that they may act as an oxidant sink. Human A8 and A9 are induced in neovessels at inflammatory sites (47) and are readily *S*-nitrosylated, and A8-SNO may modulate blood vessel homeostasis (48). Hence, changes in intracellular/extracellular redox are likely to regulate their functional properties. Moreover, their dependence on IL-10 for induction in activated human monocytes/macrophages by TLR-3 and -4 ligands (26) and their enhanced expression in various cells by anti-inflammatory agents such as corticosteroids (25) implicates A8 and A9 in resolution of inflammation.

*S*-Glutathionylation is a reversible modification that can regulate functions of numerous proteins (9, 72) including signaling and adhesion molecules, cytokines, and enzymes associated with inflammation (for review, see Ref. 14). Thus, glutathionylation of A8 and/or A9, particularly after phagocyte activation, may have important regulatory implications. However, A9 is expressed in two forms in neutrophils due to an alternate translation start site encoding Met<sup>5</sup> (56), and truncated A9\* (A9<sub>5–114</sub>) lacks the single Cys present in full-length A9 (Fig. 2*A*). Relative expression levels of these isoforms may be important because they are likely to have some functional distinctions, particularly as A9\* would not be *S*-glutathionylated or *S*-nitrosylated. We first determined the relative levels of these isoforms in neutrophil cytosol and established that full-length A9 composed  $\sim$ 70% and A9\* composed  $\sim$ 30% of total A9.

*S*-Glutathionylated adducts of recombinant A8 and A9 were generated by GSNO or GSSG *in vitro* and confirmed by ESI-MS; Ca<sup>2+</sup> or Zn<sup>2+</sup> did not alter reactivity. Formation was reversed by GSH (not shown). Glutathionylation with GSSG likely occurred via thiol-disulfide exchange as proposed (74). GSNO generated *S*-nitrosylated and *S*-glutathionylated A8 (48), and because GSNO can promote *S*-glutathionylation via *S*-nitrosothiol intermediates (75), we tested this possibility and confirmed generation of A9-SSG (Fig. 1*B*).

Neutrophil activation generates superoxides via the NADPH oxidase complex, subsequently producing other ROS (76). Early studies of *S*-thiolated proteins in PMA-activated neutrophils using Tran<sup>35</sup>S-labeling demonstrated an  $\sim$ 3–5% *S*-thiolation, predominantly glutathionylation, of a 14-kDa protein that increased over 30 min activation and was reduced by dithiothreitol. This is likely to be A9 because the protein was described as "the most abundant band in neutrophil extracts" (21). To analyze modifications of A8 and A9 after neutrophil activation, cytosolic proteins were separated by HPLC and analyzed by ESI-MS. Products likely corresponding to A9-SSG were generated by PMA or PMA plus ionomycin stimulation (Fig. 3, *B* and *C*), whereas none was separated from unstimulated cell lysates. Little co-localization of A9 with GSH was obvious in unstimulated neutrophils (Fig. 4*A*) but increased after PMA plus ionomycin stimulation (Fig. 4*B*), suggesting A9-SSG complexes. A9-SSG was not detected in the cytosol of neutrophils activated with opsonized zymosan or fMLP (Table

## S100A9 Is Glutathionylated in Neutrophils after Activation

2), although in opsonized zymosan-activated cells, A9 and GSH co-localized around the plasma membrane and possibly the phagosomal membrane (Fig. 4D). Similarly, A9 associates with neutrophil phagosomes after phagocytosis of antibody- and complement-coated latex beads (77). Thus, A9 may associate with GSH in particular cell compartments. Little co-localization of A9 with GSH was obvious in neutrophils activated with fMLP (Fig. 4C), consistent with the apparent absence of A9-SSG in cytosol extracts from this population. Apart from actin (21), the subcellular localization of glutathione-protein adducts in activated neutrophils is virtually unexplored, although studies in other cells indicate their presence in various compartments (for review, see Ref. 78). Our data suggest that A9-SSG may be generated in particular compartments depending on the stimulus and may have functional differences that warrant further investigation.

Because of its relative abundance and stability, we focused on structural characterization and functional consequences of A9 glutathionylation. This modification did not alter its  $\text{Ca}^{2+}$  or  $\text{Zn}^{2+}$  binding affinities, although conformational changes indicated increased surface hydrophobicity upon  $\text{Zn}^{2+}$  binding (Fig. 5). Thus, in certain microenvironments, particularly after neutrophil activation that promotes A9 translocation from the cytosol to the membrane, glutathionylation of A9 may facilitate interactions with lipid environments within membranes (64) or with other hydrophobic components such as fatty acids (79). In a preliminary attempt to assess the ability of A8 and A9 to form complexes using cross-linking, we found that A9-SSG may have reduced capacity to form the heterocomplex but may preferentially form more higher order A9 homocomplexes (not shown). Several intracellular functions are dependent on A8/A9 heterocomplex formation (53, 80), and differences in the  $\text{Zn}^{2+}$ -bound conformation of A9-SSG and its propensity to form homocomplexes are likely to alter function. To test this, we examined AA binding (53) but found that binding capacities of A8/A9 and A8/A9-SSG were similar.

Formation of thiol disulfides may protect key proteins including A9 from forming irreversible Cys adducts such as sulfenic and sulfonic acid derivatives during oxidative stress (81). This may be particularly relevant given that A9 is secreted (30) or passively released by dying neutrophils (31) into the extracellular inflammatory environment (82–83), which is substantially more oxidizing.

A8 and A9 mediate leukocyte migration to inflammatory sites (84–85). They are released from neutrophils during inflammatory responses induced by lipopolysaccharide (85), IL-1 $\beta$ , and tumor necrosis factor (30, 86) and chemoattractants such as activated complement, C5a, and fMLP (87). A8/A9 is deposited on the inflamed endothelium by transmigrating leukocytes (69–70) and may promote leukocyte-endothelial cell interactions (88). A9, but not the A8/A9 complex, is reported to promote neutrophil adhesion via  $\beta$ 2 integrins (32, 37) and to bind (69, 71) and activate endothelial cells (50). However, contrary to previous reports (32, 37, 68), we found no significant induction and/or activation of CD11b or CD18 ( $\alpha$ M $\beta$ 2 subset of  $\beta$ 2 integrins) on neutrophils stimulated with A9 or A9-SSG (Fig. 6A). Large variations in leukocyte responses to A9 or A9-SSG stimulation were observed between donors and could

have contributed to the discrepancies; neutrophils from 3–6 donors responded to A9 in the reported fashion, but glutathionylation had no effect.

Neutrophil adhesion to the extracellular matrix is essential for neutrophil migration, particularly of the extravasated population (89). A9 increases neutrophil adhesion to fibronectin (37), a process predominantly mediated by interactions of  $\beta$ 1 and  $\beta$ 3 integrins with extracellular matrix proteins (89), although an alternate  $\beta$ 2 integrin subset is implicated in A9-mediated responses (37). We confirmed that neutrophils stimulated with A9 or A8/A9 were significantly more adherent to fibronectin, to levels comparable with fMLP; A9-SSG promoted somewhat higher adhesion (Fig. 6B). In marked contrast, adhesion of A8/A9-SSG-treated neutrophils was not significantly different from control values (Fig. 6B). Differences in reactivity of the A8/A9-SSG heterocomplexes may be due to conformational changes, and A8 was required for negative regulation. Results here infer that the A8/A9-SSG complex may limit neutrophil migration in the extravascular compartment, another protective process that could limit the extent of inflammatory exudates. Moreover, significantly less A9-SSG and A8/A9-SSG bound endothelial cells compared with the unmodified forms (Fig. 7A). However, in contrast to earlier studies (50), we found no significant induction of ICAM-1, VCAM-1, or IL-8 mRNA in HMEC-1 stimulated with A9, A9-SSG, A8/A9, or A8/A9-SSG over 6 (Fig. 7B), 12, or 24 h (not shown). A9 also affects endothelial cell integrity and transendothelial resistance, possibly by disrupting intracellular junctions (50), and the effects of A9-SSG are worthy of investigation.

Several additional A9 modifications were observed. Similar to the generation of disulfide-linked A8 in opsonized zymosan-activated neutrophils (90), this treatment may produce disulfide-linked A9 (Table 2), likely via HOCl and/or  $\text{H}_2\text{O}_2$  oxidation, as these oxidants generated similar modifications in previous studies (43, 91). Thus, particular stimulants that produce different levels/types of ROS may determine the oxidative changes in the S100 proteins.

Products with mass similar to phosphorylated A9 were detected in fMLP- and opsonized zymosan-treated neutrophils (Table 2), consistent with earlier reports of Thr<sup>113</sup>-phosphorylated A9 and A9\* in neutrophils and monocytes activated with fMLP (92, 93). Unexpectedly, this was not found in ionomycin-stimulated neutrophils (23). A mass addition of 97 Da, detected in A9 from PMA-treated neutrophils (Fig. 3B, Table 1), may correspond to phosphorylated A9 (+80 Da) containing methionine sulfoxide (+16 Da). Mass additions of 16 and 33 Da, likely corresponding to Met oxidation to methionine sulfoxide or sulfone in A9, were consistently detected in PMA-, ionomycin-, and fMLP-treated neutrophils (Tables 1 and 2). Although beyond the scope of this study, these modifications are likely to have important functional consequences (94). Met residues on the surface of some proteins are exceptionally susceptible to oxidation and are considered oxidant scavengers (95). Oxidation to methionine sulfoxides in some proteins such as human immunodeficiency virus-2 protease (96) and  $\beta$ -amyloid peptide (97) alters their activity, and this can be readily reversed by methionine sulfoxide reductases (Msr) (98), which are highly

expressed in neutrophils (99). Full-length human A9 contains five Met residues (Met<sup>5</sup>, Met<sup>63</sup>, Met<sup>81</sup>, Met<sup>83</sup>, and Met<sup>94</sup>), and their oxidation regulates some functions; Ala substitution of Met<sup>63</sup> or Met<sup>83</sup> in A9 abrogated its antifungal activity (73) but preserved its fugetactic activity (45). Because of its abundance, Met oxidation of A9 may act as a buffer to protect other proteins from oxidative modifications in neutrophil cytosol. On the other hand, further oxidation to Met sulfone is a rare modification described in few proteins to date and is considered irreversible (100).

Generation of distinct modifications after neutrophil activation may occur via different activation pathways that produce various intensities and duration of the oxidative burst (101) and can be mediated by different mechanisms, possibly dependent on one- or two-electron oxidation (94). These modifications may regulate particular functions of A9 at different stages of the inflammatory response. Phosphorylated A9, generated during neutrophil activation by receptor-mediated agonists such as fMLP, may mediate translocation of A8/A9 from the cytosol to the plasma membrane and cytoskeleton (93) and facilitate secretion (87). On the other hand, prolonged and intense NADPH oxidase activity such as that reproduced in PMA-treated neutrophils (76, 101) may generate A9-SSG, and we propose that A9-SSG is likely released after necrosis and may contribute to the reduction of excessive extravascular neutrophil accumulation. Taken together with the ability of A8-SNO to reduce leukocyte transmigration (48), our results support the proposal that oxidative modifications together with the well accepted structural interactions between A8 and A9 may be critical in regulating the magnitude of neutrophil migration in inflammation and contribute to its resolution.

## REFERENCES

- Smith, J. A. (1994) *J. Leukocyte Biol.* **56**, 672–686
- Hampton, M. B., Kettle, A. J., and Winterbourn, C. C. (1998) *Blood* **92**, 3007–3017
- Ryter, S. W., Kim, H. P., Hoetzel, A., Park, J. W., Nakahira, K., Wang, X., and Choi, A. M. (2007) *Antioxid. Redox Signal.* **9**, 49–89
- Hultqvist, M., Olsson, L. M., Gelderman, K. A., and Holmdahl, R. (2009) *Trends Immunol.* **30**, 201–208
- Niwa, T. (2007) *J. Chromatogr. B Analyt. Technol. Biomed. Life Sci.* **855**, 59–65
- Richie, J. P., Jr., Skowronski, L., Abraham, P., and Leutzinger, Y. (1996) *Clin. Chem.* **42**, 64–70
- Giustarini, D., Rossi, R., Milzani, A., Colombo, R., and Dalle-Donne, I. (2004) *J. Cell. Mol. Med.* **8**, 201–212
- Ghezzi, P., Romines, B., Fratelli, M., Eberini, I., Gianazza, E., Casagrande, S., Laragione, T., Mengozzi, M., Herzenberg, L. A., and Herzenberg, L. A. (2002) *Mol. Immunol.* **38**, 773–780
- Dalle-Donne, I., Rossi, R., Giustarini, D., Colombo, R., and Milzani, A. (2007) *Free Radic. Biol. Med.* **43**, 883–898
- Lind, C., Gerdes, R., Hammell, Y., Schuppe-Koistinen, I., von Löwenhielm, H. B., Holmgren, A., and Cotgreave, I. A. (2002) *Arch. Biochem. Biophys.* **406**, 229–240
- Fratelli, M., Demol, H., Puype, M., Casagrande, S., Eberini, I., Salmons, M., Bonetto, V., Mengozzi, M., Duffieux, F., Miclet, E., Bachi, A., Vandekerckhove, J., Gianazza, E., and Ghezzi, P. (2002) *Proc. Natl. Acad. Sci. U.S.A.* **99**, 3505–3510
- Ghezzi, P. (2005) *Free Radic. Res.* **39**, 573–580
- Holmgren, A., Johansson, C., Berndt, C., Lönn, M. E., Hudemann, C., and Lillig, C. H. (2005) *Biochem. Soc. Trans.* **33**, 1375–1377
- Shelton, M. D., and Mieyal, J. J. (2008) *Mol. Cells* **25**, 332–346
- Niwa, T., Naito, C., Mawjood, A. H., and Imai, K. (2000) *Clin. Chem.* **46**, 82–88
- Al-Abed, Y., VanPatten, S., Li, H., Lawson, J. A., FitzGerald, G. A., Manogue, K. R., and Bucala, R. (2001) *Mol. Med.* **7**, 619–623
- Piemonte, F., Pastore, A., Tozzi, G., Tagliacozzi, D., Santorelli, F. M., Carrozzo, R., Casali, C., Damiano, M., Federici, G., and Bertini, E. (2001) *Eur. J. Clin. Invest.* **31**, 1007–1011
- Ravichandran, V., Seres, T., Moriguchi, T., Thomas, J. A., and Johnston, R. B., Jr. (1994) *J. Biol. Chem.* **269**, 25010–25015
- Pineda-Molina, E., Klatt, P., Vázquez, J., Marina, A., García de Lacoba, M., Pérez-Sala, D., and Lamas, S. (2001) *Biochemistry* **40**, 14134–14142
- Qanungo, S., Starke, D. W., Pai, H. V., Mieyal, J. J., and Nieminen, A. L. (2007) *J. Biol. Chem.* **282**, 18427–18436
- Chai, Y. C., Ashraf, S. S., Rokutan, K., Johnston, R. B., Jr., and Thomas, J. A. (1994) *Arch. Biochem. Biophys.* **310**, 273–281
- Fiaschi, T., Cozzi, G., Raugei, G., Formigli, L., Ramponi, G., and Chiarugi, P. (2006) *J. Biol. Chem.* **281**, 22983–22991
- Edgeworth, J., Gorman, M., Bennett, R., Freemont, P., and Hogg, N. (1991) *J. Biol. Chem.* **266**, 7706–7713
- Berntzen, H. B., and Fagerhol, M. K. (1990) *Scand. J. Clin. Lab. Invest.* **50**, 769–774
- Hsu, K., Passey, R. J., Endoh, Y., Rahimi, F., Youssef, P., Yen, T., and Geczy, C. L. (2005) *J. Immunol.* **174**, 2318–2326
- Endoh, Y., Chung, Y. M., Clark, I. A., Geczy, C. L., and Hsu, K. (2009) *J. Immunol.* **182**, 2258–2268
- Xu, K., Yen, T., and Geczy, C. L. (2001) *J. Immunol.* **166**, 6358–6366
- Grimbaldeston, M. A., Geczy, C. L., Tedla, N., Finlay-Jones, J. J., and Hart, P. H. (2003) *J. Invest. Dermatol.* **121**, 1168–1174
- Eckert, R. L., Broome, A. M., Ruse, M., Robinson, N., Ryan, D., and Lee, K. (2004) *J. Invest. Dermatol.* **123**, 23–33
- Rammes, A., Roth, J., Goebeler, M., Klempt, M., Hartmann, M., and Sorg, C. (1997) *J. Biol. Chem.* **272**, 9496–9502
- Voganatsi, A., Panyutich, A., Miyasaki, K. T., and Murthy, R. K. (2001) *J. Leukocyte Biol.* **70**, 130–134
- Ryckman, C., Vandal, K., Rouleau, P., Talbot, M., and Tessier, P. A. (2003) *J. Immunol.* **170**, 3233–3242
- Sohnle, P. G., Collins-Lech, C., and Wiessner, J. H. (1991) *J. Infect. Dis.* **163**, 187–192
- Miyasaki, K. T., Bodeau, A. L., Murthy, A. R., and Lehrer, R. I. (1993) *J. Dent. Res.* **72**, 517–523
- Yui, S., Mikami, M., and Yamazaki, M. (1995) *J. Leukocyte Biol.* **58**, 650–658
- Ghavami, S., Kerkhoff, C., Los, M., Hashemi, M., Sorg, C., and Karami-Tehrani, F. (2004) *J. Leukocyte Biol.* **76**, 169–175
- Anceriz, N., Vandal, K., and Tessier, P. A. (2007) *Biochem. Biophys. Res. Commun.* **354**, 84–89
- De Lorenzo, B. H., Godoy, L. C., Novaes e Brite, R. R., Pagano, R. L., Amorim-Dias, M. A., Grosso, D. M., Lopes, J. D., and Mariano, M. (2009) *Immunobiology* **215**, 341–347
- Vogl, T., Tenbrock, K., Ludwig, S., Leukert, N., Ehrhardt, C., van Zoelen, M. A., Nacken, W., Foell, D., van der Poll, T., Sorg, C., and Roth, J. (2007) *Nat. Med.* **13**, 1042–1049
- Klempt, M., Melkonyan, H., Nacken, W., Wiesmann, D., Holtkemper, U., and Sorg, C. (1997) *FEBS Lett.* **408**, 81–84
- Kerkhoff, C., Nacken, W., Benedyk, M., Dagher, M. C., Sopalla, C., and Doussiere, J. (2005) *FASEB J.* **19**, 467–469
- Vogl, T., Ludwig, S., Goebeler, M., Strey, A., Thorey, I. S., Reichelt, R., Foell, D., Gerke, V., Manitz, M. P., Nacken, W., Werner, S., Sorg, C., and Roth, J. (2004) *Blood* **104**, 4260–4268
- Harrison, C. A., Raftery, M. J., Walsh, J., Alewood, P., Iismaa, S. E., Thliveris, S., and Geczy, C. L. (1999) *J. Biol. Chem.* **274**, 8561–8569
- Raftery, M. J., Yang, Z., Valenzuela, S. M., and Geczy, C. L. (2001) *J. Biol. Chem.* **276**, 33393–33401
- Sroussi, H. Y., Berline, J., and Palefsky, J. M. (2007) *J. Leukocyte Biol.* **81**, 818–824
- Sroussi, H. Y., Berline, J., Dazin, P., Green, P., and Palefsky, J. M. (2006) *J. Dent. Res.* **85**, 829–833
- McCormick, M. M., Rahimi, F., Bobryshev, Y. V., Gaus, K., Zreiqat, H.,

## S100A9 Is Glutathionylated in Neutrophils after Activation

- Cai, H., Lord, R. S., and Geczy, C. L. (2005) *J. Biol. Chem.* **280**, 41521–41529
48. Lim, S. Y., Raftery, M., Cai, H., Hsu, K., Yan, W. X., Hsieh, H. L., Watts, R. N., Richardson, D., Thomas, S., Perry, M., and Geczy, C. L. (2008) *J. Immunol.* **181**, 5627–5636
49. Yen, T., Harrison, C. A., Devery, J. M., Leong, S., Iismaa, S. E., Yoshimura, T., and Geczy, C. L. (1997) *Blood* **90**, 4812–4821
50. Viemann, D., Strey, A., Janning, A., Jurk, K., Klimmek, K., Vogl, T., Hirono, K., Ichida, F., Foell, D., Kehrel, B., Gerke, V., Sorg, C., and Roth, J. (2005) *Blood* **105**, 2955–2962
51. Iismaa, S. E., Hu, S., Kocher, M., Lackmann, M., Harrison, C. A., Thliveris, S., and Geczy, C. L. (1994) *DNA Cell Biol.* **13**, 183–192
52. Markert, M., Cech, P., and Frei, J. (1984) *Blut* **49**, 447–455
53. Kerkhoff, C., Klempt, M., Kaefer, V., and Sorg, C. (1999) *J. Biol. Chem.* **274**, 32672–32679
54. Atienza, J. M., Yu, N., Kirstein, S. L., Xi, B., Wang, X., Xu, X., and Abassi, Y. A. (2006) *Assay Drug Dev. Technol.* **4**, 597–607
55. Eue, I., König, S., Pior, J., and Sorg, C. (2002) *Int. Immunol.* **14**, 287–297
56. Teigelkamp, S., Bhardwaj, R. S., Roth, J., Meinardus-Hager, G., Karas, M., and Sorg, C. (1991) *J. Biol. Chem.* **266**, 13462–13467
57. Kerkhoff, C., Klempt, M., and Sorg, C. (1998) *Biochim. Biophys. Acta* **1448**, 200–211
58. Edgeworth, J., Freemont, P., and Hogg, N. (1989) *Nature* **342**, 189–192
59. Roth, J., Burwinkel, F., van den Bos, C., Goebeler, M., Vollmer, E., and Sorg, C. (1993) *Blood* **82**, 1875–1883
60. Lemarchand, P., Vaglio, M., Mauël, J., and Markert, M. (1992) *J. Biol. Chem.* **267**, 19379–19382
61. Roulin, K., Hagens, G., Hotz, R., Saurat, J. H., Veerkamp, J. H., and Siegenthaler, G. (1999) *Exp. Cell Res.* **247**, 410–421
62. Hessian, P. A., Edgeworth, J., and Hogg, N. (1993) *J. Leukocyte Biol.* **53**, 197–204
63. Meister, A., and Anderson, M. E. (1983) *Annu. Rev. Biochem.* **52**, 711–760
64. van den Bos, C., Roth, J., Koch, H. G., Hartmann, M., and Sorg, C. (1996) *J. Immunol.* **156**, 1247–1254
65. Zhukova, L., Zhukov, I., Bal, W., and Wyslouch-Cieszyńska, A. (2004) *Biochim. Biophys. Acta* **1742**, 191–201
66. Goch, G., Vdovenko, S., Kozłowska, H., and Bierzyński, A. (2005) *FEBS J.* **272**, 2557–2565
67. Kerkhoff, C., Vogl, T., Nacken, W., Sopalla, C., and Sorg, C. (1999) *FEBS Lett.* **460**, 134–138
68. Newton, R. A., and Hogg, N. (1998) *J. Immunol.* **160**, 1427–1435
69. Robinson, M. J., Tessier, P., Poulosom, R., and Hogg, N. (2002) *J. Biol. Chem.* **277**, 3658–3665
70. Hogg, N., Allen, C., and Edgeworth, J. (1989) *Eur. J. Immunol.* **19**, 1053–1061
71. Srikrishna, G., Panneerselvam, K., Westphal, V., Abraham, V., Varki, A., and Freeze, H. H. (2001) *J. Immunol.* **166**, 4678–4688
72. Klatt, P., and Lamas, S. (2000) *Eur. J. Biochem.* **267**, 4928–4944
73. Sroussi, H. Y., Köhler, G. A., Agabian, N., Villines, D., and Palefsky, J. M. (2009) *FEMS Immunol. Med. Microbiol.* **55**, 55–61
74. Gallogly, M. M., and Mieyal, J. J. (2007) *Curr. Opin. Pharmacol.* **7**, 381–391
75. Giustarini, D., Milzani, A., Aldini, G., Carini, M., Rossi, R., and Dalle-Donne, I. (2005) *Antioxid. Redox Signal.* **7**, 930–939
76. El-Benna, J., Dang, P. M., Gougerot-Pocidallo, M. A., and Elbim, C. (2005) *Arch. Immunol. Ther. Exp. (Warsz)* **53**, 199–206
77. Burlak, C., Whitney, A. R., Mead, D. J., Hackstadt, T., and Deleo, F. R. (2006) *Mol. Cell. Proteomics* **5**, 620–634
78. Martínez-Ruiz, A., and Lamas, S. (2007) *Cardiovasc. Res.* **75**, 220–228
79. Siegenthaler, G., Roulin, K., Chatellard-Gruaz, D., Hotz, R., Saurat, J. H., Hellman, U., and Hagens, G. (1997) *J. Biol. Chem.* **272**, 9371–9377
80. Leukert, N., Vogl, T., Strupat, K., Reichelt, R., Sorg, C., and Roth, J. (2006) *J. Mol. Biol.* **359**, 961–972
81. Poole, L. B., Karplus, P. A., and Claiborne, A. (2004) *Annu. Rev. Pharmacol. Toxicol.* **44**, 325–347
82. Kocher, M., Kenny, P. A., Farram, E., Abdul Majid, K. B., Finlay-Jones, J. J., and Geczy, C. L. (1996) *Infect. Immun.* **64**, 1342–1350
83. Corbin, B. D., Seeley, E. H., Raab, A., Feldmann, J., Miller, M. R., Torres, V. J., Anderson, K. L., Dattilo, B. M., Dunman, P. M., Gerads, R., Caprioli, R. M., Nacken, W., Chazin, W. J., and Skaar, E. P. (2008) *Science* **319**, 962–965
84. Herndon, B. L., Abbasi, S., Bennett, D., and Bamberger, D. (2003) *J. Lab. Clin. Med.* **141**, 110–120
85. Vandal, K., Rouleau, P., Boivin, A., Ryckman, C., Talbot, M., and Tessier, P. A. (2003) *J. Immunol.* **171**, 2602–2609
86. Kido, J., Hayashi, N., Kataoka, M., and Nagata, T. (2005) *J. Periodontol.* **76**, 437–442
87. Hetland, G., Talgö, G. J., and Fagerhol, M. K. (1998) *Mol. Pathol.* **51**, 143–148
88. Kerkhoff, C., Eue, I., and Sorg, C. (1999) *Pathobiology* **67**, 230–232
89. Lindbom, L., and Werr, J. (2002) *Semin. Immunol.* **14**, 115–121
90. Kumar, R. K., Yang, Z., Bilson, S., Thliveris, S., Cooke, B. E., and Geczy, C. L. (2001) *J. Leukocyte Biol.* **70**, 59–64
91. Rahimi, F., Hsu, K., Endoh, Y., and Geczy, C. L. (2005) *FEBS J.* **272**, 2811–2827
92. Bengis-Garber, C., and Gruener, N. (1993) *J. Leukocyte Biol.* **54**, 114–118
93. Lominadze, G., Rane, M. J., Merchant, M., Cai, J., Ward, R. A., and McLeish, K. R. (2005) *J. Immunol.* **174**, 7257–7267
94. Schöneich, C. (2005) *Biochim. Biophys. Acta* **1703**, 111–119
95. Levine, R. L., Mosoni, L., Berlett, B. S., and Stadtman, E. R. (1996) *Proc. Natl. Acad. Sci. U.S.A.* **93**, 15036–15040
96. Davis, D. A., Newcomb, F. M., Moskovitz, J., Fales, H. M., Levine, R. L., and Yarchoan, R. (2002) *Methods Enzymol.* **348**, 249–259
97. Hou, L., Shao, H., Zhang, Y., Li, H., Menon, N. K., Neuhaus, E. B., Brewer, J. M., Byeon, I. J., Ray, D. G., Vitek, M. P., Iwashita, T., Makula, R. A., Przybyla, A. B., and Zagorski, M. G. (2004) *J. Am. Chem. Soc.* **126**, 1992–2005
98. Moskovitz, J. (2005) *Biochim. Biophys. Acta* **1703**, 213–219
99. Achilli, C., Ciana, A., Rossi, A., Balduini, C., and Minetti, G. (2008) *J. Leukocyte Biol.* **83**, 181–189
100. Vogt, W. (1995) *Free Radic. Biol. Med.* **18**, 93–105
101. Decoursey, T. E., and Ligeti, E. (2005) *Cell. Mol. Life Sci.* **62**, 2173–2193